Eur. Phys. J. B **39**, 219–227 (2004)
DOI: 10.1140/epjb/e2004-00184-y

THE EUROPEAN PHYSICAL JOURNAL B

Two-step spin conversion and other effects in the atom-phonon coupling model

J.A. Nasser[1,a], K. Boukheddaden[2], and J. Linares[2]

[1] Laboratoire LIRIS, Université de Versailles Saint-Quentin, 45 avenue des États-Unis, 78035 Versailles Cedex, France
[2] Laboratoire de Magnétisme et d'Optique, CNRS-UMR 8634, Université de Versailles Saint-Quentin, 45 avenue des États-Unis, 78035 Versailles Cedex, France

Received 2 February 2004
Published online 29 June 2004 –

Abstract. We study an atom-phonon coupling model introduced recently for spin-conversion phenomenon. The originality of this model, performed on a linear chain of atoms, is that the elastic force constant values of the spring linking two atoms depends on their electronic states. This leads to introduce naturally in the chain long- and short-range interactions, which appear respectively like a Zeeman and an exchange interactions. The exchange-like interaction can be ferro-, antiferro- or equal to zero. The effects of long-range interactions have already been studied. Here we study those of the short-range interaction. Some parts of the chain phase diagram are analysed and the main features of the experimental behaviours of spin conversion compounds are qualitatively reproduced.

PACS. 63.20.Kr Phonon-electron and phonon-phonon interactions – 63.50.+x Vibrational states in disordered systems – 64.60.-i General studies of phase transitions

1 Introduction

The first case of spin conversion (SC) reported in the literature is due to Cambi in 1931 [1]. Since then, many experimental and theoretical studies have been done [2,9]. Recently, the effects of hydrostatic pressure [10], applied magnetic field [11] and light [12] have been studied on (SC) compounds. In addition, spin transition phenomenon has been observed on compounds with a strong one dimensional character [13].

The (SC) compound is constituted of transition metal ions in an octahedral environnement. Due to the metallic ion ligand field and spin pairing energy, the transition metal energy diagram displays a fundamental level with a spin value less than that of the first excited level. For example, for iron(II) complexes, the low spin value is $S = 0$ and the high spin one is $S = 2$. Moreover, for these complexes, the fundamental energy level is non degenerated, whereas the degeneracy of the excited energy level is the product of the spin and orbital degeneracies. When the orbital moment is completely quenched, the degeneracy of the excited level becomes equal to $(2S + 1)$.

Mössbauer-effect studies and magnetic susceptibility measurements allow to study the thermal variation of the high-spin fraction, n_{HS}, that is the fraction of transition metal in the high spin level. This parameter deviates from a Boltzmann population law and can display two different behaviours: (i) either n_{HS} increases continuously with increasing temperature and does not show a thermal hysteresis; (ii) or n_{HS} shows with increasing temperature a discontinuity and a thermal hysteresis, which is characteristic of a first order phase transition (called spin transition). Recently, it has been shown that the first order phase transition can disappear and reappear when hydrostatic pressure is applied [13]. In some compounds [14], a "two-steps" spin-conversion can be observed with or without first order phase transition. In such spin conversion, the high spin fraction increases very smoothly in a range of temperature of few kelvin.

Let Δ be the distance in energy between the fundamental and the first excited level of the transition metal. The experimental studies show that n_{HS} is near of the unit for a temperature value T_{sat} less than Δ (typically, Δ is near of two or three times kT_{sat}, where k is Boltzmann constant). So, it is clear that there is a mechanism which helps the transition metal ions to go from the low spin level to the high spin one. Which is this mechanism?

Different mechanisms have been proposed [4] to [8], [15] and [16]. For example, in the Ising-like model [15], an exchange-like interaction is introduced, but the physical origin of this interaction is not specified. Moreover the exchange-like constants and the degeneracy of the high-spin level are determined in order to have a good fit with

[a] e-mail: jnasser@physique.uvsq.fr

the experimental results. Hence, in order to reduce the value of the parameter T_{sat}, a very high value is given to the degeneracy of the high level, typically 1000. This high value cannot be due to the above mentioned electronic degeneracy alone. So, degeneracy related to the vibrations of the atoms complexes is assumed.

Recently [18], starting from the experimental results obtained by Sorai and Seki [17], Nasser assumed that acoustic phonons are this driving force. He proposed a 1-D model in which spin-conversion units, represented by simple atoms with fictitious two-states spins, are coupled by springs such as the elastic force constant of a spring has three values depending on the electronic states of both atoms linked by the spring. The three values are chosen such as to favour the high spin level. So, the thermal variation of the high spin fraction results from the competition between the electronic parameter Δ which favours the low spin level, and the acoustic phonons of the lattice.

In his paper, Nasser shows that phonon system creates a field-like on each atom and an exchange-like interaction between two first-neighbouring atoms. This exchange-like interaction can be ferro-, antiferro- or even equal to zero. Only the case where the exchange-like interaction is zero has been studied [18]. In that case, the field-like leads the chain to have a spin conversion with or without a first order transition depending on the respective values of elastic force constant. Moreover, the ratio between the parameters Δ and T_{sat} is acceptable even for the electronic degeneracy alone.

In this paper, we look for the new results due to the antiferro- exchange-like interaction. By the same variational method as that used in [18], we can separate the chain Hamiltonian in two parts: a phonon Hamiltonian and a spin one. In order to preserve the character 1-D of the system, the spin Hamiltonian is studied with the transfer matrix method.

The aim of this study is to investigate the chain phase diagram and to obtain for the high spin fraction thermal variation behaviours which look like to those obtained by experimental studies.

In Section 2 we present the model and the chain Hamiltonian, in Section 3 we describe the study method used, in Section 4 we give the obtained results and the last section is devoted to discussion and conclusion.

2 The model and the chain Hamiltonian

Let us consider a linear chain of identical atoms having two energy levels. The degeneracy of the fundamental electronic level (a) is $g_a = 1$ and that of the excited level (b) is $g_b = r$. We call Δ the difference in energy between the two levels. Neighbouring atoms i and j $(= i \pm 1)$ are assumed to interact with an elastic force constant e_{ij}, which is equal to λ when both atoms are in level (a), ν when they are both in (b) and μ when one is in level (a) and the other in level (b). We assume that

$$\lambda > \mu > \nu. \tag{1}$$

To each atom i, $(i = 1$ to N), we associate a fictitious-spin $\hat{\sigma_i}$ which has two eigen-values $\sigma_i = \pm 1$. Eigen-value -1 (resp.$+1$) corresponds to electronic level (a) (resp. (b)).

The total Hamiltonian of the chain is the sum:

$$H = H_{spin} + H_{phonon} \tag{2}$$

where the spin Hamiltonian H_{spin} is

$$H_{spin} = \sum_{i=1}^{N} \frac{\Delta}{2} \hat{\sigma}_i \tag{3}$$

and H_{phonon}, the phonon Hamiltonian, is

$$H_{phonon} = E_c + E_p. \tag{4}$$

E_c is the total kinetic energy of the chain and E_p its elastic potential energy. The latter can be written as

$$E_p = \sum_{i=1}^{N} \frac{1}{2} e_{i,i+1} q_i^2 \tag{5}$$

with

$$q_i = u_{i+1} - u_i \tag{6}$$

and

$$e_{i,i+1} = \frac{\lambda + 2\mu + \nu}{4} + 2h_0(\hat{\sigma}_i + \hat{\sigma}_{i+1}) \; + 2J_0 \hat{\sigma}_i \hat{\sigma}_{i+1} \tag{7}$$

with

$$h_0 = \frac{\nu - \lambda}{8} \tag{8}$$

and

$$J_0 = \frac{\lambda - 2\mu + \nu}{8}. \tag{9}$$

In these expressions, u_i is the displacement of the ith atom from its equilibrium position which we assume to be independent of the electronic states of the atoms. Moreover we assume the periodic condition, $u_{p+N} = u_p$ for $p = 1, 2, \ldots, N$.

The chain potential energy, E_p, can be decomposed as

$$E_p = V_0 + V_1 + V_2 \tag{10}$$

with

$$V_0 = \sum_{i=1}^{N} \frac{\lambda + \nu + 2\mu}{8} q_i^2 \tag{11}$$

$$V_1 = \sum_{i=1}^{N} h_0 \left[q_{i-1}^2 + q_i^2 \right] \hat{\sigma}_i \tag{12}$$

and

$$V_2 = \sum_{i=1}^{N} J_0 q_i^2 \hat{\sigma}_i \hat{\sigma}_{i+1}. \tag{13}$$

The energy V_1 is the sum of one-spin interactions, it has Zeeman-like form. Each spin $\hat{\sigma}_i$ is submitted to an effective field h_i given by

$$h_i = h_0 \left[q_{i-1}^2 + q_i^2 \right]. \tag{14}$$

From the hypothesis $\nu < \lambda$, this field favours the eigen value +1 ((b) level).

The energy V_2 is the sum of two-spin interactions, it has an exchange-like form. The exchange parameter J_{ii+1} between spin σ_i and σ_{i+1} is

$$J_{ii+1} = J_0 q_i^2 \tag{15}$$

The sign of this parameter is the same as that of the expression J_0. For example, when J_{ii+1} is negative, V_2 is a ferromagnetic-like interaction.

In a previous article [18], the case $V_2 = 0$, that is $J_0 = 0$, has been studied. In the present work we study the influence of the V_2 term on the chain phase diagram.

3 Effective elastic force constant K and transfer matrix

3.1 Self-consistent equations

If we replace the elastic force constant $e_{i,i+1}$ by an effective elastic force constant K which does not depend on the chain sites, then the thermal mean value of the parameter q_i does not depend on the site i. So, the field, h_i (Eq. (14)), created by the phonon on spins is uniform along the chain, and moreover the exchange parameter, $J_{i,i+1}$ (Eq. (15)), is the same between any couple of first neighbours spins. We then obtain a spin Hamiltonian which can be studied exactly by the transfer matrix method [19].

We can obtain the best expressions for the effective elastic constant, K, for the effective uniform field, h, and for the effective exchange-like interaction, J, by a variational method [20]. The variational Hamiltonian H_0 is given by:

$$H_0 = H_{0s}(h, J) + H_{0ph}(K) \tag{16}$$

with

$$H_{0s} = \sum_{i=1}^{N} -h\hat{\sigma}_i + \sum_{i=1}^{N} -J\hat{\sigma}_i\hat{\sigma}_{i+1} \tag{17}$$

and

$$H_{0ph}(K) = \sum_{i=1}^{N} \frac{p_i^2}{2m} + \sum_{i=1}^{N} \frac{K}{2} q_i^2. \tag{18}$$

As the parameters h and J do not depend on the sites, the Hamiltonian H_{0s} can studied exactly. Using the transfer matrix method we obtain for F_{0s}, the free energy related to H_{0s},

$$F_{0s} = -NkT\frac{\ln r}{2} - NkT \ln A \tag{19}$$

with

$$A = \exp(\beta J)\cosh\beta h_r + \sqrt{B} \tag{20}$$

and

$$B = \exp(2\beta J)\sinh^2\beta h_r + \exp(-2\beta J). \tag{21}$$

In the above relations, kT is the thermal energy, $\beta = \frac{1}{kT}$ and

$$h_r = h + kT\frac{\ln r}{2} \tag{22}$$

The relation (22) takes into account the degeneracy of the excited level (or b level).

In the case of the Hamiltonian H_{0s} the thermal mean values of $\hat{\sigma}_i$, and that of $\hat{\sigma}_i\hat{\sigma}_{i+1}$ are independent on the site i. So, we introduce the parameters m and s defined by

$$m = \langle\hat{\sigma}_i\rangle \text{ for } i = 1, N \tag{23}$$

and

$$s = \langle\hat{\sigma}_i\hat{\sigma}_{i+1}\rangle \text{ for } i = 1, N. \tag{24}$$

It is known that the transfer matrix method leads to equations

$$m = \frac{\exp(\beta J)\sinh\beta h_r}{\sqrt{B}} \tag{25}$$

and

$$s = 1 - \frac{2\exp(-2\beta J)}{A\sqrt{B}}. \tag{26}$$

The expression of F_{0ph}, the free energy related to the phonon Hamiltonian, $H_{0ph}(K)$, is well known. It is given by

$$F_{0ph} = kT\sum_{\alpha} \ln\left(2\sinh\beta\frac{\hbar\omega_\alpha}{2}\right) \tag{27}$$

where $\sum_\alpha$ is the sum over phonon normal modes. The frequencies are given by

$$\omega_\alpha = \omega_M(K) \mid \sin\frac{\alpha\pi}{N} \mid \tag{28}$$

where $\alpha = 0, \pm1, \pm2, ..., \pm(\frac{N}{2} - 1), \frac{N}{2}$. The maximum frequency is given by

$$\omega_M(K) = 2\sqrt{\frac{K}{m_a}} \tag{29}$$

where the parameter m_a is the atoms mass.

The variational free energy is then

$$\tilde{F} = F_0 + \langle H - H_0\rangle_0 \tag{30}$$

where

$$F_0 = F_{0s} + F_{0ph} \tag{31}$$

and $\langle H - H_0\rangle_0$ is the thermal mean value calculated by using the density matrix associated to H_0 at temperature T.

The minimization of $\tilde{F}$ versus the variational parameters h, J and K, leads to the equations:

$$K = \frac{2\mu + \lambda + \nu}{4} + 4h_0 m + 2J_0 s \tag{32}$$

$$h = -\frac{\Delta}{2} - \frac{2h_0}{K}\frac{\langle H_{0ph}(K)\rangle_T}{N} \tag{33}$$

$$J = -\frac{J_0}{K}\frac{\langle H_{0ph}(K)\rangle_T}{N}. \tag{34}$$

Up to now, we have only taken into account one phonon polarisation. For simplicity, we assume that the phonon energy is independent of the polarisation. Then,

taking into account the three polarisations, we must multiply by three the phonon energy in the expressions of h and J. So, equations (33) and (34) become

$$h = -\frac{\Delta}{2} - 6\frac{h_0}{K}\frac{\langle H_{0ph}(K)\rangle_T}{N} \tag{35}$$

$$J = -3\frac{J_0}{K}\frac{\langle H_{0ph}(K)\rangle_T}{N}. \tag{36}$$

Inserting the expressions of h, J and K given by equations (32, 35) and (36) in $\tilde{F}$, we obtain F, the chain free-energy corresponding to the approximation made in this study. The expression of F is given in Appendix A.

When the parameters λ, μ, ν and r are fixed, F appears as a function of Δ, T, s and m. However, as m and s verify two self consistent equations then the free energy F is only function of Δ and T. The expression of the free energy differential and that of the chain entropy are given in Appendix A.

3.2 Chain isotherms study

To numerically solve the self consistent equations, we take $\hbar\omega_M(\lambda)$ as the unit of energy and we introduce the following reduced parameters:

- the reduced temperature:

$$t = \frac{kT}{\hbar\omega_M(\lambda)} \tag{37}$$

- the dimensionless electronic excitation energy

$$\delta = \frac{\Delta}{\hbar\omega_M(\lambda)} \tag{38}$$

- the elastic force constant ratio

$$x = \frac{\nu}{\lambda}. \tag{39}$$

We have assumed that $0 < x < 1$.

- the dimensionless parameter y defined by:

$$\mu = \frac{\lambda+\nu}{2} + \frac{\lambda-\nu}{2}y \tag{40}$$

It is clear that the parameter y is the ratio

$$y = \frac{J_0}{h_0}. \tag{41}$$

Due to the assumption made on the elastic constant values (Eq. (1)) the parameter y must verify the conditions

$$-1 < y < 1. \tag{42}$$

We have studied the chain isotherms in the Δ-m plane. From the isotherms study we can deduce the chain phase diagram in the δ-t plane or in the δ-y plane.

In this article we have restricted the study of the chain phase diagram for the case where the exchange-like interaction is anti-ferro, that is for

$$\mu < \frac{\lambda+\mu}{2} \Longleftrightarrow y < 0. \tag{43}$$

This case is interesting because there is then a competition between the Zeeman-like interaction which makes the spin parallel and the anti-ferro exchange-like interaction which makes them anti-parallel. Moreover, we have limited the chain phase diagram study to the case $x = 0.2$ for which the Zeeman-like interaction leads the chain to display a first order phase transition at any temperature value [18].

4 Results

4.1 Chain phase diagram at 0 K

At 0 K, the self-consistent equations can be solved exactly which provides a guide in the choice of the parameters values for the numerical study at $T \neq 0$ K. At 0 K three solutions can be found:

a) $m = 1$ and $s = 1$, corresponding to a pure high-spin phase (HS). The elastic constant of this phase is equal to ν, and its energy, E_+, is given by

$$E_+ = 3\langle H_{0ph}(\nu)\rangle_{0\ \mathrm{K}} + N\frac{\Delta}{2}. \tag{44}$$

b) $m = -1$ and $s = 1$, corresponding to a pure low-spin phase (LS). The elastic constant of this phase is equal to λ and its energy, E_-, is given by

$$E_- = 3\langle H_{0ph}(\lambda)\rangle_{0\ \mathrm{K}} - N\frac{\Delta}{2}. \tag{45}$$

c) $m = 0$ and $s = -1$, corresponding to a pure antiferro phase (AF). The elastic constant of this phase is equal to μ and its energy, $E_\pm$, is given by

$$E_\pm = 3\langle H_{0ph}(\mu)\rangle_{0\ \mathrm{K}}. \tag{46}$$

In these expressions, $\langle H_{0ph}(\nu)\rangle_{0\ \mathrm{K}}$, $\langle H_{0ph}(\lambda)\rangle_{0\ \mathrm{K}}$ and $\langle H_{0ph}(\mu)\rangle_{0\ \mathrm{K}}$ are the zero-point energies of the chain with the respective elastic force constants ν, λ and μ.

We can show that when N, the number of chain atoms, tends to infinity the zero-point energy of a periodic chain is given by

$$\langle H_{ph}(e)\rangle_{0\ \mathrm{K}} = N\frac{2}{\pi}\frac{\hbar\omega_M(e)}{2}. \tag{47}$$

In the above relation e is the elastic force constant of the chain and $\omega_M(e)$ is its maximum phonon frequency.

Between the three solutions, the stable one is that which has the lowest energy value. So, at 0 K, the chain phase diagram can be deduced from the energy (E) diagram studied in the E-Δ plane.

Since we have assumed $\nu < \mu < \lambda$, then, for $\Delta = 0$, the value of E_+ is less than those of E_- and of $E_\pm$, and the value of $E_\pm$ lies between those of E_+ and of E_-.

As shown in the relation (44, 45), E_+ increases linearly and E_- decreases linearly as Δ increases. As for $E_\pm$, it does not depend on Δ but decreases when the parameter μ decreases.

From the above results, we deduce that, when $\Delta = 0$, the chain is in the (HS) phase. When Δ increases two cases must be considered:

– a) if the value of μ is near of that of λ, then, for $\Delta = 0$, the value of $E_\pm$ is near of that of E_-. In this case, the chain displays a first order phase transition between the (HS) and the (LS) phases. Indeed, at some particular value of Δ, which we denote by Δ_1, the energies of the two phases are equal. And, when $\Delta < \Delta_1$ the (HS) solution is the stable phase while the stable phase is the (LS) solution for $\Delta > \Delta_1$. The expression of Δ_1 is obtained from the relation

$$E_+(\Delta_1) = E_-(\Delta_1). \tag{48}$$

Using (47), we find

$$\Delta_1 = \frac{3}{\pi}(\hbar\omega_M(\lambda) - \hbar\omega_M(\nu)) \tag{49}$$

– b) if the value of μ is near of that of ν, then, for $\Delta = 0$, the value of $E_\pm$ is near of that of E_+. In this case, as Δ increases, the chain displays a first order phase transition between the (HS) and the (AF) phases at the particular value Δ_2 followed by a first order phase transition between the (AF) and the (LS) phases at the particular value Δ_3. The expressions of Δ_2 and Δ_3 verify the equations

$$E_+(\Delta_2) = E_\pm(\Delta_2) \tag{50}$$

and

$$E_\pm(\Delta_3) = E_-(\Delta_3). \tag{51}$$

Using (47), the values Δ_2 and Δ_3 are then given by

$$\Delta_2 = \frac{6}{\pi}(\hbar\omega_M(\mu) - \hbar\omega_M(\nu)) \tag{52}$$

and

$$\Delta_3 = \frac{6}{\pi}(\hbar\omega_M(\lambda) - \hbar\omega_M(\mu)). \tag{53}$$

It is clear that the values Δ_2 and Δ_3 depend on the value of the parameter μ. One can verify that both values are equal to Δ_1 for a particular value of μ, which we designate as μ_s. Using the relations (52) or (53), the value of μ_s is given by

$$\hbar\omega_M(\mu_s) = \frac{\hbar\omega_M(\lambda) + \hbar\omega_M(\nu)}{2}. \tag{54}$$

Using the relation (29) in (54), we obtain

$$\sqrt{\frac{\mu_s}{\lambda}} = \frac{1+\sqrt{x}}{2}. \tag{55}$$

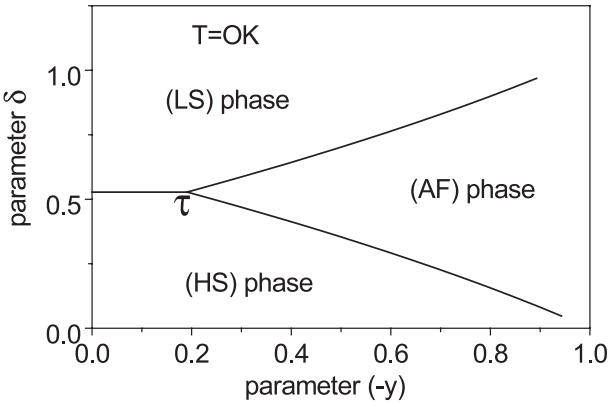

Fig. 1. Chain phase diagram at 0 K for $x = 0$. The full lines are the coexistence curves of two phases. The coordinates of the triple point τ are $\delta_\tau = 0.52787$ and $y_\tau = -0.19098$. For $y = 0.0$, $\delta = 0.52787$. The parameter δ is the reduced ligand field parameter, x is the ratio of the elastic constant values for HS-HS and LS-LS pair, y characterizes the difference between elastic constant value for the pair HS-LS and the mean value of the elastic constants HS-HS and LS-LS.

One can show that μ_s is a threshold value. Indeed, if $\mu > \mu_s$, the chain is that of case a), and if $\mu < \mu_s$ it is in the case b). Moreover, since the three phases energies are equal for $\mu = \mu_s$ and $\Delta = \Delta_s$, then the chain phase diagram displays a triple point at 0 K.

From the relations (40) and (55), the value y_s of the reduced parameter y for $\mu = \mu_s$ is

$$y_s = \frac{-(1+x) + 2\sqrt{x}}{2(1-x)} \tag{56}$$

for $x = 0.2$, $y_s = -0.19098$.

In Appendix A we give the expressions of the reduced values δ_i (i=1,2,3) in terms of the reduced parameters x and y.

The previous results are summarized in the chain phase diagram at 0 K, shown in Figure 1. It is worth noticing that r, the excited level degenerency value, does not play any role in this phase diagram.

4.2 Chain phase diagram for T ≠ 0 K

For $T \neq 0$ K, we have studied the chain isotherms by solving numerically the self consistent equations (25, 26). We have limited ourselves to study the cases $x = 0.2$, $r = 5$ and $y < 0$.

Here, we first give a general property verified by the self consistent equations, and then we present some aspects of the chain phase diagram.

From the equations (22, 35) and (36) it appears that fixing the value of the temperature and that of the phonon parameters λ, μ and ν, the parameters h_r and J do not change if we replace the set of values ($\Delta = \Delta_1$ and $r = r_1$)

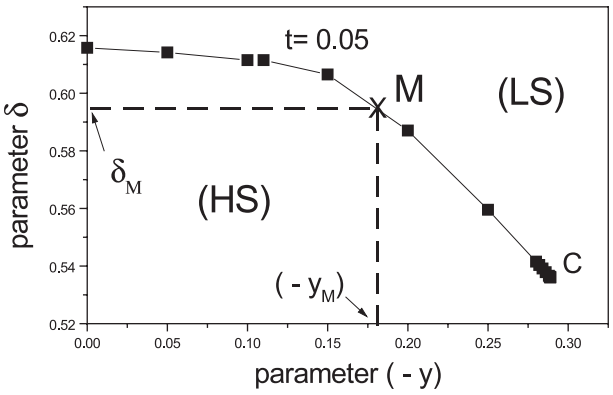

Fig. 2. Chain phase diagram at $t = 0.05$, for $x = 0.2$ and $N = 2000$. The line is the (HS) phase-(LS) phase coexistence curve. The coordinates of the critical point C are $t_C = 0.05$, $y_C = -0.2889$ and $\delta_C = 0.5361$. Below the transition line the phase is (HS), above it, the phase is (LS), but not a pure (LS) phase (see the text). The parameter t is the reduced temperature.

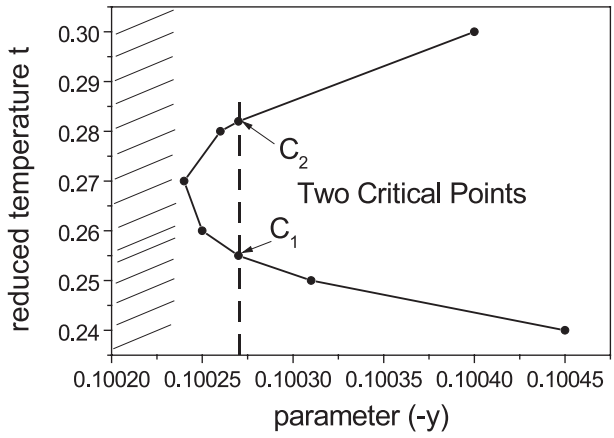

Fig. 3. Line of the chain critical points in the t-$(-y)$ plane; $x = 0.2$ and $N = 2000$. Let $-y_C$ and t_C be the coordinates of each critical point. The minimum value of $(-y_C)$ is higher than 0.1 but very close to this value. The dashed area goes from $y = 0$ to the minimum value of $(-y_C)$. For a fixed value of $(-y)$, the chain phase diagram in the δ-t plane doesn't display a critical point in the dashed zone, but, in the white zone, such phase diagram displays two critical points denoted C_1 and C_2 in the figure. Their coordinates are respectively $t_{C_1} = 0.255$, $y_{C_1} = -0.10027$, $\delta_{C_1} = 1.0556$ and $t_{C_2} = 0.282$, $y_{C_2} = -0.10027$ and $\delta_{C_2} = 1.1344$.

by any set ($\Delta = \Delta_2$ and $r = r_2$) such as

$$kT \ln r_1 - \Delta_1 = kT \ln r_2 - \Delta_2. \tag{57}$$

Therefore, the solutions of the self-consistent equations (25, 26) are the same for the set (Δ_1, r_1) and the set (Δ_2, r_2) related by the relation (57). So, studying the chain isotherms for $r = r_1$, allows us to deduce the isotherms for any value of r by using the transformation (57).

For $t = 0.02$, the chain phase diagram in the δ-$(-y)$ plane is similar to that at 0 K. However, it is no more the case at higher temperature values.

The chain phase diagram, in the δ- $(-y)$ plane, at $t = 0.05$, is shown in Figure 2. This phase diagram displays only one first order phase transition line ended by a critical point C. Let y_C, δ_C and t_C be the coordinates of this critical point.

In Figure 2, let δ_M and $-y_M$ be the coordinates of a point M of the transition line, and suppose δ to be increased, maintaining $(-y)$ constant at the value $-y_M$. For δ values less than or greater than δ_M the self consistent equations solution is a unique set of two values one for m and one for s. Let (m_1, s_1) be the self consistent equations solution for the value δ_- just less than δ_M, and let (m_2, s_2) be the solution for the value δ_+ just greater than δ_M. As the point M is on a first order phase transition line, $m_1 \neq m_2$ and $s_1 \neq s_2$. We have verified that $m_1 > m_2$ for any position of the point M on the transition line. For this reason, we say that the phase below the transition line is a (HS) phase, and that above the transition line is a (LS) phase. However, while the phase below the transition line is nearly a pure (HS) phase, with $m_1 > 0.72$ and $s_1 > 0.448$ for $0 < (-y) < (-y_C)$, it is not the case for the phase above the transition line. Indeed,

- for $0 < (-y) < 0.11$, this phase is quite a pure (LS) phase with $m_2 < 0$ and $s_2 > 0$;
- for $0.15 < (-y) < 0.2$, this phase looks like an (AF) phase, with $s_2 < 0$ and $m_2 \simeq 0$;
- for $0.28 < (-y) < y_C$, this phase can be considered as a (HS) phase less ordered than the (HS) phase below the transition line. Indeed, in this case, m_2 and s_2 are positive.

We have followed the thermal variations of the critical values $(-y_C)$ and δ_C. The value δ_C is a monotonous increasing function of the temperature. As for $(-y_C)$, when the temperature increases, this value first decreases, reaches a minimum value and then increases. The variations of $(-y_C)$ vs. t_C, near the minimum is shown in Figure 3.

We have verified by numerical calculation that, in the range of temperature where $(-y_C)$ decreases, that is at low temperature, the chain free-energy is positive and decreases, while, in the range where $(-y_C)$ increases, the chain free-energy is negative and decreases. So we can say that the thermal behaviour of $(-y_C)$ is due to the competition between internal energy and entropy terms of the chain free-energy.

From Figure 3, we deduce that when we fix the value of the parameter $(-y)$ at a value less than the minimum value of $(-y_C)$ the chain phase diagram in the δ-t plane does not display a critical point. However, if the value of $(-y)$ is larger than this minimum value, this phase diagram displays two critical points called C_1 and C_2 in Figure 3.

The chain phase diagram in the δ-t plane for $y = -0.10027$ is shown in Figure 4.

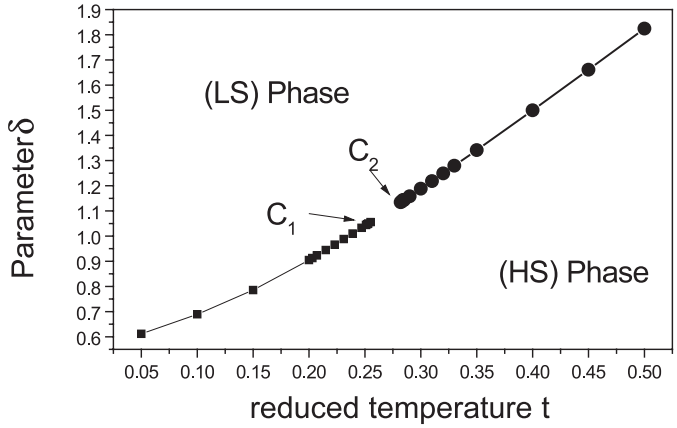

Fig. 4. Chain phase diagram for $y = -0.10027$; $x = 0.2$ and $N = 2000$. The full line is the coexistence curve of the (HS) and (LS) phases. This curve is interrupted between the critical points C_1 and C_2 which are those of Figure 3. For δ values between δ_{C_1} and δ_{C_2} the chain doesn't display a first order phase transition.

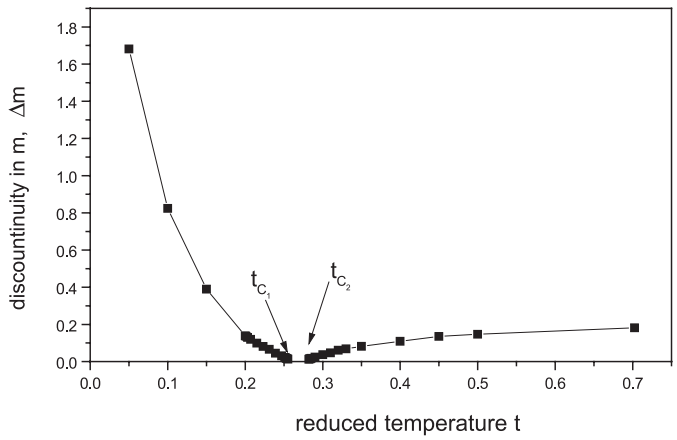

Fig. 5. Values of Δm, the discontinuity in m, along the coexistence curve of Figure 4. When the transition temperature value tends to the critical temperature values t_{C_1} or t_{C_2}, Δm tends to zero. When the transition temperature value is very small, Δm is large, but when the temperature transition increases, being larger than t_{C_2}, Δm tends to a constant value near of 0.2.

The slope of the coexistence curve is given by the Clapeyron equation

$$\frac{d(\frac{\Delta}{2})}{dT} = \frac{\Delta S}{\Delta m} \tag{58}$$

where ΔS and Δm are the discontinuities at the transition of the entropy and of the parameter m respectively. The values of Δm for the different temperature values of the coexistence curve of Figure 4 are shown in Figure 5.

Using reduced parameters δ and t in the Clapeyron equation we deduced ΔS, the value of the entropy discontinuity per mole at the transition

$$\Delta S = \frac{R}{2}\Delta m \frac{d\delta}{dt} \tag{59}$$

where R is the perfect gas constant. Using the above relation and the results contained in Figures 4 and 5, one can calculate ΔS. In our numerical study, we can calculate the entropy of each solution of the self-consistent equations, and then, we deduce the entropy discontinuity without using the above relation.

4.3 Thermal variation of the high-spin fraction

In the experimental studies, the physicists measure the thermal variation of the high-spin fraction which is related to the "magnetization" m through the relation

$$n_{hs} = \frac{1+m}{2}. \tag{60}$$

To have, in our study, the thermal variation of the high-spin fraction we fix the values of the model parameters λ, μ, ν, Δ and r and we solve the self-consistent equations for different temperature values.

When the spin conversion takes place through a first order phase transition our numerical study shows the existence of thermal hysteresis. However, the calculated thermal hysteresis can't be compared to the observed one. So, in this study, we only display the stable solutions, and then the first order phase transition appears through a discontinuity in the spin fraction at the transition temperature.

Using the chain phase diagram displayed in Figure 4, we predict that the thermal variation of the high spin fraction is continuous for a δ value between δ_{C_1} and δ_{C_2} and is discontinuous for a δ value less than δ_{C_1} or bigger than δ_{C_2}. Those results are shown in Figure 6.

When the parameter y is small enough, the chain phase diagram displays in the δ-t plane, an anti-ferro phase, that is a phase where $s < 0$ and $m \approx 0$. This phase is limited by two first order transition lines each ended by a critical point. Consequently, if we choose for δ a value just greater than the δ values of the above mentioned critical points, we obtain for the high spin fraction thermal variation the behaviour shown in Figure 7. This behaviour looks like that called "unusual spin-transition anomaly" or "two-step spin conversion" by H. Köppen et al. [14].

5 Discussion and conclusion

The phase diagram of Figure 4 is surprising. However, it allows to understand the results obtained by Yann Garcia et al. [13] in studying pressure effect on a 1D spin conversion compound. Their results are the following: the thermal variation of n_{HS} displays a thermal hysteresis at atmospheric pressure, and, as the applied pressure increases, the hysteresis width decreases, disappears and again reappears with a constant width.

If we assume that the ligand field parameter Δ (or δ) increases when the applied pressure increases, we can interpret the experimental results of Garcia et al. by saying that the first order phase transition disappears and reappears when the compound parameter Δ increases, which

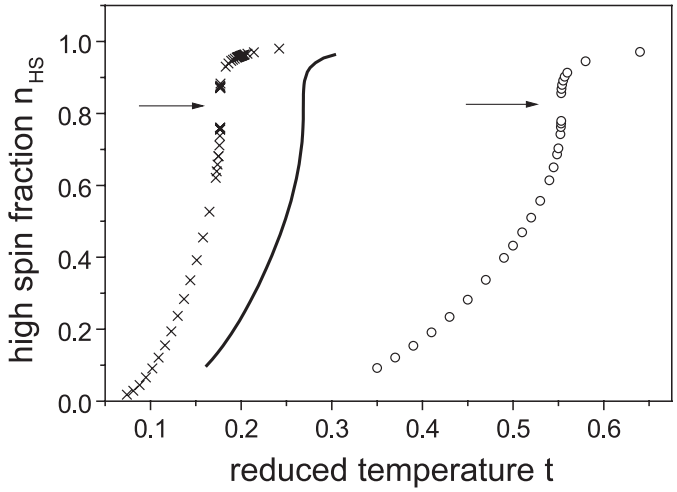

Fig. 6. Thermal variation of the high spin fraction for $x = 0.2$, $r = 5$, $y = -0.10027$, $N = 2000$ for different values of δ. For $\delta = 0.847$, that is $\delta < \delta_{C_1}$, symbol (×), the chain displays a first order transition at the temperature value of 0.1769. For $\delta = 1.095$, that is $\delta_{C_1} < \delta < \delta_{C2}$, (full line), the spin conversion is continuous. For $\delta = 2.0$, that is $\delta > \delta_{C_2}$, symbol (o), the chain displays again a first order transition. The discontinuities in n_{HS} are indicated by arrows.

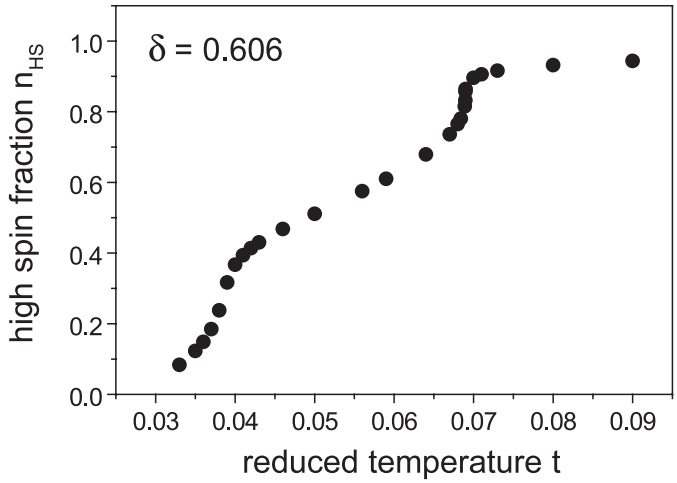

Fig. 7. Thermal variation of the high spin fraction for $x = 0.2$, $r = 5$, $y = -0.20$, $\delta = 0.606$ and $N = 2000$. In the "plateau region", the chain is in an anti-ferro phase. This high spin thermal variation is similar to the experimental curves called "unusual spin-transition anomaly" or "two-steps" spin transition.

is the results showed in Figure 6. In other words, one can say that the value of δ in the compound studied by Garcia et al. is equal to a value less than the critical value δ_{C_1} at atmospheric pressure, belongs to the range $(\delta_{C_1}, \delta_{C_2})$ at 4.1 kbar and is greater than δ_{C_2} when the applied pressure is greater than or equal to 5 kbar. It is worth noticing that, in the model, for $\delta > \delta_{C_2}$, the discontinuity in m at the transition is nearly constant. This result, shown in Figure 5, may be the reason why the observed hysteresis width has a constant value when the applied pressure is greater than or equal to 5 kbar.

For $\delta = 0.847$ and $r = 5$, (symbol ×) in Figure 6, we have obtained, by solving the self-consistent equations, 0.1769 for the reduced value of the transition temperature, $\Delta m = 0.218$ for the discontinuity in m and $\Delta S = 0.264$ R for the discontinuity in the chain entropy. It is worth noticing that using Figures 4 and 5 and the Clapeyron equation we can deduce the value of the entropy discontinuity at the transition. For example, if we choose the value 0.1 for the reduced transition temperature, we obtain by this way 0.8 R for the entropy discontinuity at the transition. (The energy unit of the model, $\hbar\omega_{\mathrm{M}}(\lambda)$, is of the order of 1000 K, so a reduced temperature value of 0.1 corresponds to 100 K).

For $r = 15$ and $\delta = 0.847$, we have obtained by solving the self-consistent equation the values 0.1167 for the reduced transition temperature and 0.906 R for the entropy discontinuity at the transition.

For the spin transition shown in Figure 6 (symbol ×) we have calculated ΔS_{12}, the chain entropy variation between a temperature value t_1, less than the transition temperature, and a temperature value t_2, greater than it. We have found: $\Delta S_{12} = 1.7$ R for $t_1 = 0.158$ and $t_2 = 0.195$; and $\Delta S_{12} = 2.5$ R for $t_1 = 0.137$ and $t_2 = 0.212$.

Garcia et al. [13] have obtained 32.2 $\mathrm{J\,mol^{-1}\,K^{-1}}$ or 3.87 R for the entropy variation. This value cannot be compared with the entropy discontinuity values obtained in the present model because of the observed thermal hysteresis.

From our study, we can conclude that the present atom-phonon coupling model allows us to reproduce qualitatively the thermal behaviours of the high spin fraction observed in spin conversion compounds. However, as shown in Figures 6 and 7, the range of temperature containing the thermal variation of the high spin fraction is too large compared to the observed temperature range. We think that taking into account the thermal variation of the parameter Δ can reduce the calculated temperature range.

In this study, working on a 1-D system, we have been able to use the transfer matrix method to investigate the role of the exchange-like interaction. But if we try to apply this atom-phonon coupling model on a 2-D or 3-D system, we will be obliged to replace the transfer matrix method by a molecular field theory which is less correct. However, in this case, this study on a 1-D system could help for choosing the model parameters values.

As an extension of the present work, we project in a near future to study the dynamical properties of this model.

Finally, one of us, J.A. Nasser is indebted to L. Chassagne for helpful discussions.

Appendix A

A.1 Chain thermodynamic function

In the used approximation, F, the chain free-energy is

$$F = -NkT\left(\frac{\ln r}{2} + \ln A\right) + 3kT\sum_{\alpha}\ln\left(2\sinh\beta\frac{\hbar\omega_{\alpha}}{2}\right) + N\left(\frac{\Delta}{2} + h\right)m + NJs. \quad (61)$$

The meaning of the different parameters are contained in Section 3.1.

A.2 Chain free-energy differential and entropy

Taking the infinitesimal variation of F, we find

$$dF = -SdT + Nmd\frac{\Delta}{2} \quad (62)$$

where S, the chain entropy, is given by

$$S = S_{spin} + S_{ph} \quad (63)$$

with

$$S_{spin} = -N\frac{h\,m + Js}{T} + Nk\ln A + Nk\frac{\ln r}{2} \quad (64)$$

and

$$S_{ph} = \frac{3\langle H_{0ph}(K)\rangle}{T} - 3k\sum_{\alpha}\ln\left(2\sinh\beta\frac{\hbar\omega_{\alpha}}{2}\right). \quad (65)$$

The spin entropy is that of N spin (± 1) interacting with first neighbour exchange interaction and submitted to the applied field h. The phonon entropy is that of a periodic chain with elastic force of constant K.

A.3 Transition lines equations at 0 K

In order to do calculation, we use the reduced parameters introduced in (37) to (40). The expressions of the reduced values δ_i for $i = 1, 2, 3$ are the following:

$$\delta_1 = \frac{3}{\pi}\left(1 - \sqrt{x}\right) \quad (66)$$

$$\delta_2 = \frac{6}{\pi}\left(\sqrt{\frac{1+x}{2} + \frac{1-x}{2}y} - \sqrt{x}\right) \quad (67)$$

and

$$\delta_3 = \frac{6}{\pi}\left(1 - \sqrt{\frac{1+x}{2} + \frac{1-x}{2}y}\right). \quad (68)$$

References

1. L. Cambi, A. Cagnasso, Atti. Accad. Naz. Lincei **13**, 809 (1931)
2. E. König, G. Ritter, S.K. Kulshreshtha, Chem. Rev. **85**, 219 (1985)
3. C.P. Köhler, R. Jakobi, E. Meissner, L. Wiehl, H. Spiering, P. Gütlich, J. Phys. Chem. Solids **51**, 239 (1990)
4. R.A. Bari, J. Sivardière, Phys. Rev. B **5**, 4466 (1972)
5. T.J. Kambara, J. Chem. Phys. **70**, 4199 (1979)
6. R. Zimmermann, E. König JPCS **38**, 779 (1977)
7. J. Wajnflasz, Phys. Stat. Solidi **40**, 537 (1970); J. Wajnflasz, R. Pick, J. Phys. France **32**, C1-91 (1971)
8. N. Willebacher, H. Spiering, J. Phys. C **21**, 1423 (1988)
9. R. Boca, M. Boca, H. Ehrenberg, H. Fuess, W. Linert, F. Renz, I. Svoboda, Chem. Phys. **293**, 375 (2003)
10. F. Varret, A. Bleuzen, K. Boukheddaden, A. Bousseksou, E. Codjovi, C. Enachescu, A. Goujon, J. Linares, N. Menendez, M. Verdageur, Pure Appl. Chem. **74**, 2093 (2002)
11. A. Bousseksou, K. Boukheddaden, M. Goiran, C. Consejo, M.-L. Boillot, J.-P. Tuchagues, Phys. Rev. B **65**, 172412 (2002)
12. P. Gütlich, A. Hauser, H. Spiering, Angw. Chem. Int. Ed. Engl. **33**, 2024 (1994)
13. Y. Garcia, V. Ksenofontov, G. Levchenko, P. Gütlich, Roy. Soc. Chem. **10**, 2274 (2000)
14. H. Köppen, E.W. Müller, C.P. Köhler, H. Spiering, E. Meissner, P. Gütlich, Chem. Phys. Lett. **91**, 348 (1982)
15. A. Bousseksou, J. Nasser, J. Linares, K. Boukheddaden, F. Varret, J. Phys. I France **2**, 1381 (1992)
16. R. Boca, M. Boca, L. Dihan, K. Falk, H. Fuess, W. Haase, R. Jarosciak, B. Papankova, F. Renz, M. Vrbova, R. Werner, Inorg. Chem. **40**, 3025 (2001)
17. M. Sorai, S. Seki, J. Phys. Chem. Solids **35**, 555 (1974)
18. J.A. Nasser, Eur. Phys. J. B **21**, 3 (2001)
19. J.M. Yeomans, *Statistical Mechanics of Phase Transitions* (Oxford University Press, 1992)
20. R. Balian, *Microphysics to Macrophysics. Methods and Applications of Statistical Physics* (Berlin Heidelberg New York, Springer-Verlag, 1991), Vol. 1